High-Throughput Screening of Drug−Brain Tissue Binding and in Silico Prediction for Assessment of Central Nervous System Drug Delivery

Hong Wan,*,† Mikael Rehngren,‡ Fabrizio Giordanetto,§ Fredrik Bergström,† and Anders Tunek‡

Lead Generation DMPK & Physical Chemistry, Lead Generation Computational Chemistry, Discovery DMPK and Bioanalytical Chemistry, AstraZeneca R&D, Mölndal, SE-431 88, Mölndal, Sweden

Received March 29, 2007

A high-throughput method for rapid screening of in vitro drug−brain homogenate binding is presented. The method is based on a straightforward sample pooling approach combining equilibrium dialysis with liquid chromatography mass spectrometry (LCMS). A strong correlation of fraction unbound in brain (f_u) between single compound measurements and 25-pooled compounds ($R^2 = 0.906$) was obtained for a selection of structurally diverse CNS compounds with a wide range of fractions unbound. Effects of brain homogenate dilution and dialysis time were investigated. To the best of our knowledge, it was the first time that we have demonstrated consistent fraction unbound in mouse and rat brain homogenate, revealing the drug−tissue partitioning mechanism predominated by hydrophobic interaction. On the basis of this finding, a generic approach to estimate drug binding to various tissues is proposed. A robust and interpretable QSAR for f_u prediction is also presented by statistical modeling.

1. Introduction

Achieving a high extent of central nervous system (CNS) exposure is an important focus for CNS drug discovery.[1,2] Brain to plasma ratio (K_p) has been widely used in CNS drug discovery to indicate whether a drug has good brain penetration. Also, many computational models employ K_p or log BB (log ratio of blood to brain) as a key parameter to assess brain permeation.[3−8] However, the relevance for pharmacodynamics of blood−brain barrier penetration as expressed by log BB has been questioned.[9,10] Recent studies have clearly demonstrated that a compound such as sulpiride, having a K_p value as low as 0.15 in wild-type mice, can still be a successful CNS drug,[11] suggesting that it is difficult to assess the relevance and implications of brain penetration solely on the basis of total brain to plasma ratio (K_p) at steady state. Alternatively, it has been proposed to use unbound brain to unbound plasma ratio ($K_{p-unbound}$) to describe brain penetration, since the unbound brain to plasma ratio rather than the total brain to plasma ratio reflects a partitioning between brain and plasma, which usually is pharmacologically more relevant.[1] Summerfield et al. presented improved in vitro prediction of in vivo CNS penetration by integrating permeability, P-glycoprotin efflux, and fractions unbound in blood and brain.[13] Kalvass and co-workers recently demonstrated that the unbound brain to plasma ratio provides a simple alternative means for assessing the CNS distribution of drug independent of the mechanisms involved.[14] This is consistent with the "unbound drug hypothesis", since, for most if not all CNS targets, unbound brain concentration drives the in vivo pharmacological effect. Consequently, the determination of in vitro brain tissue binding (f_u) in connection with measurements of total exposure is indispensable to evaluate in vivo pharmacological effects as well as to assess brain penetration for CNS targets.

Currently, the main technique applied for measuring the fraction unbound in brain tissue still relies on equilibrium dialysis using brain homogenates, although several other methods have been utilized.[15] The dialysis-based assay is considered to be an accurate method for fraction unbound measurement, but it is hampered by a very low throughput. Accordingly, the development of a more high-throughput method for the screening of brain tissue binding would be highly desirable.

In this context, we present a high-throughput approach to screen brain homogenate binding which will benefit CNS-related drug discovery projects. A robust QSAR model was developed to enable to predict brain tissue binding.

2. Methods and Materials

2.1. Brain Tissue Homogenates and Sample Preparation. Brain tissue homogenate samples were prepared by diluting one volume of the whole brain tissue with three volumes of buffer (100 mM sodium phosphate, pH 7.4), and the mixture was homogenized using an ultrasound probe. Fresh brain homogenates were ready for dialysis, and the rest of the homogenates were frozen at −20 °C for later comparison. Usually, the brain tissues from three or more individual mice were pooled to obtain reproducibility in the tissue components.

A test set of commercial CNS drug compounds with a wide range of physicochemical properties was employed for this study (see Table 1). The selection of compounds was based on published data as well as in-house data from AstraZeneca (AZ). Two other compounds, verapamil and 5,5-diethyl-1,3-diphenyl-2-aminobarbituric acid, were used as volume markers in the LCMS analysis. A group of AZ compounds with one or two basic pK_a values was included for the QSAR model study. A solution consisting of 0.5 mM compound in DMSO was used as stock solutions, and 10 μL of stock solution was added to 1 mL of homogenate to yield a compound concentration of 5 μM in the homogenates. Three portions of 200 μL volume each were used for dialysis (triple samples), and 50 μL of homogenate was stored in the 96-well analysis plate in a freezer for recovery analysis later. The rest of the 350 μL was used for a stability test along with the dialysis samples. The sample pooling approach is similar to the single compound measurement by mixing of compounds in 10 mM DMSO stocks, yielding an individual compound concentration of 0.5 mM, including one reference standard (propranolol) as quality control. In the case of pooling 25 compounds, a concentration of 4 μM for each compound in the homogenate was employed.

* To whom correspondence should be addressed. Phone: +46 31 776 4801. Fax: +46 31 776 3748. E-mail: hong.wan@astrazeneca.com.
† Lead Generation DMPK & Physical Chemistry.
‡ Discovery DMPK and Bioanalytical Chemistry.
§ Lead Generation Computational Chemistry.

10.1021/jm070375w CCC: $37.00
Published on Web 08/29/2007

Table 1. List of CNS Compounds and Their Physicochemical Properties and Fractions Unbound (f_u) in Mouse and Rat Brain Tissues[a]

CNS compounds	mass	pK_a, CEMS	ClogP (C-lab)	logD7.4 (in-house)	f_u%(single):[12] mouse, 4.5 h	f_u%(pooling) mouse, 4.5 h	f_u%(pooling) rat, 4.5 h	f_u%(pooling) mouse, 20 h
buspirone	386.26	7.8	2.185	2.61	22	20 ± 1.6	16 ± 1.4	7.2 ± 0.75
carbamazepine	237.10	n	2.19	1.77	12	17 ± 1.9	16 ± 1.8	17 ± 2.8
carisoprodol	261.18	n	2.341	2.4	20	42 ± 5.4	36 ± 3.9	31 ± 6.0
chlorpromazine	319.10	9.54	5.35	3.7	0.076	0.16 ± 0.018	0.12 ± 0.024	0.11 ± 0.055
citalopram	325.17	9.72	3.132	1.94	3	3.8 ± 0.24	3.4 ± 0.099	2.8 ± 0.38
clozapine	327.14	7.93/3.79	3.714	3.46	0.94	1.2 ± 0.075	1 ± 0.17	1.13 ± 0.20
cyclobenzaprine	276.17	9.69	5.097	2.92	0.73	0.65 ± 0.044	0.58 ± 0.024	0.34 ± 0.11
diazepam	285.08	3.55	2.99	3.53	5	4.2 ± 0.64	4.3 ± 0.5	3.5 ± 0.4
fluoxetine	310.14	10.2	4.26	2.84	0.22	0.25 ± 0.027	0.26 ± 0.016	0.18 ± 0.083
fluvoxamine	319.16	9.4	3.321	2.41	0.84	0.861 ± 0.097	0.79 ± 0.030	0.81 ± 0.22
haloperidol	376.15	9.02	4.28	0.18	0.71	1 ± 0.23	0.82 ± 0.10	0.3 ± 0.12
hydrocodone	300.16	8.43	1.126	3.38	55	55 ± 6.1	52 ± 9.2	41 ± 5.7
hydroxyzine	375.18	7.75	3.995	0.18	1	1.5 ± 0.071	1.3 ± 0.16	0.81 ± 0.15
lamotrigine	256.02	5.19	2.534	0.54	22	29 ± 0.93	25 ± 1.7	18 ± 4.3
methylphenidate	234.15	9.24	2.556	-0.15	22	30 ± 3.9	27 ± 2.9	12 ± 3.2
metoclopramide	300.15	9.59	2.62	3.31	31	46 ± 7.9	35 ± 8.2	26 ± 5.3
midazolam	326.09	5.44	3.27	2.50	2.7	2.6 ± 0.25	2.5 ± 0.042	1.7 ± 0.29
nortriptyline	264.17	10.41	4.04	2.23	0.46	0.42 ± 0.039	0.36 ± 0.020	0.26 ± 0.12
paroxetine	330.15	10.1	4.238	2.27	0.39	0.26 ± 0.029	0.26 ± 0.030	0.095 ± 0.002
propranolol	260.16	9.68	2.98	1.33	1.92	2.2 ± 0.3	2.0 ± 0.19	1.3 ± 0.17
risperidone	411.22	8.63/3.16	2.711	1.66	6.7	11 ± 1.1	8.7 ± 0.9	3.9 ± 0.5
selegiline	188.14	7.69	2.9	3.7	5.6	9 ± 1.1	7.4 ± 0.45	4.5 ± 0.79
trazodone	372.16	6.73	3.85	2.97	4.7	5.8 ± 0.42	4.4 ± 0.48	3 ± 0.081
venlafaxine	278.21	9.9	3.269	0.88	21	28 ± 4.8	22 ± 4	19 ± 3.5
zolpidem	308.18	6.02	3.026	2.35	20	21 ± 3.3	17 ± 3.7	13 ± 2.0

[a] n: neutral. 4.5 h and 20 h are dialysis times. f_u%(single) is reference data[12] measured with a single compound, except for propranolol; f_u%(pooling) data were measured in this work by pooling 25 compounds.

2.2. Equilibrium Dialysis. Equilibrium dialysis was carried out on a laboratory-made chamber consisting of two symmetric plexiglass halves, a volume of 250 μL, and a semipermeable membrane with a molecular cutoff of 5 kDa (Dianorm GmbH D-81215 München, Germany) between the two halves. The membranes were first washed with water and then soaked in buffer for 30 min before being placed in the dialysis cells. A 200 μL volume of buffer was added into one side of the chamber and an equivalent volume of homogenate with spiked compounds (4−5 μM of each compound in homogenate) was added to the other side of the membrane. For comparison of the effect of dialysis time, the compounds were dialyzed 4.5 h and overnight (approximately 20 h) at 37 ± 1 °C in an air incubator. A 50 μL volume from the buffer side (representing the unbound concentration) and an equivalent sample volume from the homogenate side (representing the total concentration) were transferred from the dialysis cells to a 96-deep well plate for LCMS analysis.

2.3. HPLC Separation and Mass Spectrometry Detection. A Waters Acquity UPLC integrated LC system (Waters Sweden Inc., Sollentuna, Sweden) was used for all HPLC separations. All sample preparations were carried out on a TECAN GenMate 96 needle pipetting robot (TECAN Switzerland AG, Männedorf, Switzerland). A Waters Acquity 1.7 μm, 2.1 × 50 mm analytical column (Waters Sweden Inc.) and an HPLC gradient was used as follows. The linear gradient runs from 0 to 5 min by mixing mobile phase A (5% ACN and 95% H_2O) containing 0.2% of formic acid in deionized water and mobile phase B (95% ACN and 5% H_2O) containing 0.2% formic acid. The flow rate was 0.7 mL/min and the integrated column heater was set at 40 °C.

A Waters MicroMass LCT Premier TOF mass spectrometer (run in ESI+ and W-mode with extended dynamic range) was used for detection with the software Masslynx 4.0 and Quanlynx 4.0 for data acquisition and quantitation, respectively (Waters Sweden Inc.). Source temperature, 120 °C; desolvation temperature, 450 °C; cone gas flow, 100 L/h; desolvation gas flow, 1000 L/h; resolution, 10 000; reference scan frequency, 50; scan duration, 100 ms; and interscan delay, 20 ms.

2.4. LCMS Bioanalysis Procedure. The dialyzed samples were precipitated to remove tissue, and the supernatant was analyzed by LCMS. The following three solutions were used in the sample preparation: Solution 1: acetonitrile containing 0.1 μM of volume markers verapamil and 1.0 μM 5,5-diethyl-1,3-diphenyl-2-aminobarbituric acid. Solution 2: deionized water containing 0.2% (volume) of formic acid. Solution 3: dilution solution consisting of 150 mL of acetonitrile, 150 mL of deionized water, and 200 μL of formic acid, respectively.

Both the 50 μL of tissue homogenate and 50 μL of buffer samples were precipitated with 150 μL of cold (4 °C) solution 1. The samples were then mixed thoroughly in a multivortexer for 1 min and centrifuged at an RCF of 3220 for 20 min. A 100 μL portion of supernatant from each sample was diluted with 50 μL of solution 2. These samples are referred to as "nondiluted samples" (although the sample preparation implies a 6-fold dilution). A 25 μL volume of such nondiluted samples was then transferred to the second 96-well plate and diluted 10 times with solution 3. These samples are referred as "10-times diluted samples". A 25 μL volume of such 10-times diluted samples was further diluted another 10 times in the same way, yielding the third 96-well plate as "100-times diluted samples". All samples, i.e., the nondiluted and 10-times and 100-times diluted samples, were then analyzed by LCMS. f_u of the homogenate (f_{u-hom}) was calculated from the ratio of the buffer side response to the homogenate side responses, taking into account both linearity and dilution factors.

2.5. Calculation of Fraction Unbound (f_u), Recovery, and Stability. On the basis of a nonspecific binding relationship between drug and tissue, fraction unbound ($f_{u-tissue}$) for nondiluted tissue can be recalculated from measured f_u in homogenate (f_{u-hom}),[16,17] without the necessity of knowing the identity or exact concentrations of the tissue components, with the following equation

$$f_{u-tissue} = \frac{1/D_f}{(1/f_{u-hom} - 1) + 1/D_f} = \frac{f_{u-hom}}{D_f - (D_f - 1)f_{u-hom}} \quad (1)$$

where f_{u-hom} and D_f represent the measured fraction unbound in diluted homogenate and the dilution factor, respectively.

Recovery and stability were estimated using eqs 2 and 3:

$$\text{recovery (\%)} = 100 \times \frac{(\text{response}_{\text{hom}} + \text{response}_{\text{buffer}})_{\text{after dialysis}}}{(\text{response}_{\text{hom}})_{\text{before dialysis}}} \quad (2)$$

$$\text{stability (\%)} = 100 \times \frac{(\text{response}_{\text{hom}})_{\text{after incubation}}}{(\text{response}_{\text{hom}})_{\text{before incubation}}} \quad (3)$$

2.6. Physicochemical Property Characterization. Lipophilicity and ionization (pK_a) of all compounds in Table 1 were measured. Lipophilicty was estimated by an in-house assay based on a liquid chromatographic retention approach using a C-18 column and a gradient at pH 7.4. A group of compounds with known log *D* values was employed for calibration. The pK_a of the same set of compounds was determined by CEMS, as previously described,[18] with extended application of 14 buffers and on-line reference control for accurate pK_a screening.[19,20] In general, the pK_a values for most of the compounds are well in line with those reported in the literature,[11] but some deviations were observed. For instance, two pK_a values were observed for clozapine and risperidone, and a pK_a of 9.24 versus the reported value of 10.6 was found for methylphenidate. Midazolam (5.44), lamotrigine (5.19), and diazepam (3.55) show weak basic pK_a values, while they were reported as neutral. It should be noted that all compounds with pK_a lower than 6 could be regarded as neutral compounds, since these compounds exhibit nearly zero effective mobility at physiological pH 7.4.[19,20] However, these weak pK_a values should also be taken into account when only the nonionized form is concerned.

2.7. Statistical Modeling. A variety of structural descriptors, capturing both 2D and 3D molecular properties, were computed using in-house developed software. The Pearson correlation coefficient (*r*) was employed to reduce collinearity in the descriptor set: if *r* was higher than 0.8 for a given descriptor pair, then the descriptor that was more correlated with the unbound brain fraction (f_u) (i.e., that had the largest absolute value of *r*) was retained. Two data sets were used in the present study. The first one includes 108 compounds for which unbound brain fractions were measured in either rat or mouse and was used for general statistical analysis. The second data set is a subset of the first one and consisted of 70 compounds with f_u measured in mice. It was divided into training (65%, 56 compounds) and test (35%, 24 compounds) groups to allow QSAR model derivation and evaluation, respectively. Several data modeling techniques, developed through the R project,[21] as implemented in Pipeline Pilot,[22] were employed to build statistical models. These include multiple linear regression (MLR), partial least-squares (PLS), principal component analysis regression (PCR), neural networks (NN), and support vector machine (SVM) methods.

The internal consistency of the resulting models was evaluated with randomization tests on both dependent and independent variables and different types of cross-validation. These included leaving one, five, and 10 observations out during model building. The process was repeated 50 times in the case of leave-five and leave-ten-out schemes. External predictivity was subsequently evaluated by predicting the unbound brain fraction values for the molecules in the test set. Additional measurements performed on eight molecules after the models were built provided a further prospective test.

3. Results and Discussion

3.1. Sample Pooling Based on Reversible and Nonspecific Binding and/or Partitioning. In our previous work, we have demonstrated the suitability of sample pooling for screening drug−plasma protein binding from theoretical calculations and measurements.[23] Similar to the drug−protein binding, the drug binding to tissue can be regarded as a rapid and reversible equilibrium. Since the exact identity and concentration of nonspecific binding components in brain tissue are unknown, a nonlinear relationship between f_u and binding component concentration was used for back calculation of f_u for the original tissue[17] using eq 1. Equation 1 is derived on the basis of a one-to-one binding model similar to drug protein binding[24,25] by means of eqs 4−6.

$$[D] + [B] \Leftrightarrow [BD] \quad (4)$$

$$K_d = \frac{1}{K_a} = \frac{[D][B]}{[BD]} \quad (5)$$

$$f_u = \frac{[D]}{[D_T]} = \frac{[D]}{[D] + [BD]} = \frac{K_d}{[B] + K_d} = \frac{(\text{response})_{\text{buffer}}}{(\text{response})_{\text{tissue}}} \approx \frac{\text{aqueous phase}}{\text{organic phase}} \quad (6)$$

In these equations [D], [BD], and [D_T] are the concentrations of unbound drug, bound drug and total drug, respectively; [B] is the binding component concentration, mainly phospholipid concentration in the tissue; and K_d and K_a are the dissociation constant and the corresponding association constant, which are independent of the total drug concentration and the binding component concentration in the brain tissue.

Equation 6 implies that the fraction unbound (f_u) resembles the partitioning between aqueous phase (buffer) and organic phase (tissue lipids), being a function of the binding tissue component concentration while independent of the total drug concentration, which should be the case as long as the concentration of tissue components is in large excess. Consequently, the equilibrium of a particular compound out of pooled compounds is expected to be the same as the equilibrium for a single compound, provided that the pooled total drug concentration is still much lower than the lipid concentration. For a better understanding of the sample pooling applicability, we can also simulate the f_u in homogenates using eq 7,[25] where the f_u is associated only with the total drug [D_T] and total binding component concentrations [B_T].

$$f_u\% = 100 - \text{bound (\%)} = 100 \times \frac{(K_a[D_T] + K_a[B_T] + 1) - \sqrt{(K_a[D_T] + K_a[B_T] + 1)^2 - 4K_a^2[B_T][D_T]}}{2K_a[D_T]} \quad (7)$$

As illustrated in Figure 1, an increasing binding affinity (enhanced partitioning) results in decreased f_u in general. However, the f_u is identical in the range of drug concentration from 1 to 500 μM (case a) in 4-times diluted homogenate (assumed total lipid concentration 17.5 M; cf. Figure 1). A similar trend was obtained also for 20-times diluted homogenate (lipid concentration was 3.5 mM) as long as the total drug concentration is below 100 μM (case b). These results could be attributed largely to the fact that the lipid content in the homogenate is much greater than the drug concentration, leading to a consistent f_u independence of drug concentration. To further verify this theoretical model, and to demonstrate that sample pooling is a viable approach for drug−tissue binding screening, we conducted dilution experiments as well as the sample pooling experiments.

3.2. Effect of Homogenate Dilution on Fraction Unbound. Unlike plasma protein binding measurements, in vitro brain tissue binding has to be carried out in diluted homogenates adaptable for equilibrium dialysis. Thus, the fraction unbound measured in diluted homogenates has become questioned. Concerns have been raised that the dilution of tissue proteins and alteration of tissue binding mechanisms may limit the validity of this methodology.[15] This urged us to examine whether the dilution of brain tissue would influence the brain f_u. For the

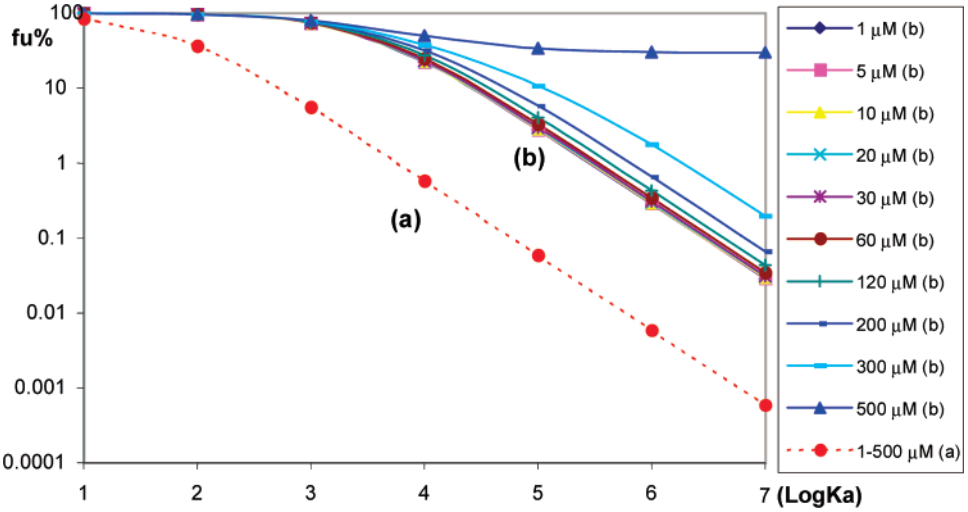

Figure 1. f_u independent of drug concentration in diluted brain homogenate. Calculations based on eq 7, where a wide range of drug concentrations from 1 to 500 μM was used. (a) four-time diluted homogenate; an assumed binding component concentration of 17.5 mM for neutral lipid and phospholipid was used for f_u calculation. (b) Twenty-time diluted homogenate, corresponding to 3.5 mM phospholipid used for f_u calculation, demonstrates that a number of compounds could be pooled with f_u independent of drug concentration from the theoretical binding model. Fractional content of wet tissue weight is 0.05 in mouse tissue and 0.053 in rat tissue.[26] Simply taking into account only the amount of phospholipids and an average molecular weight of 700 in the brain tissue, the molar concentration of phospholipids in the brain tissue is approximately 71 mM.

Table 2. Independence of f_u on Mouse Brain Tissue Homogenate Dilution[a]

	f_u%					
compound	4-times	8-times	10-times	12-times	16-times	20-times
chlorpromazine	0.11 ± 0.037	0.089 ± 0.019	0.1 ± 0.022	0.078 ± 0.024	0.074 ± 0.008	0.123 ± 0.04
haloperidol	0.28 ± 0.07	0.29 ± 0.08	0.27 ± 0.07	0.25 ± 0.097	0.23 ± 0.037	0.4 ± 0.12
diazepam	3.1 ± 0.07	1.9 ± 0.18	1.9 ± 0.41	1.4 ± 0.22	1.4 ± 0.21	1.9 ± 0.4
carisoprodol	23 ± 0.068	17 ± 1.36	18 ± 7.0	14 ± 1.96	10 ± 2	19 ± 10.8
lamotrigine	26 ± 2.3	17 ± 5.1	15 ± 3.9	14 ± 2.24	14 ± 2.52	17 ± 3.9
buspirone	5.5 ± 0.88	3.5 ± 0.31	4.2 ± 1.1	3.5 ± 0.56	3.8 ± 1.29	3.5 ± 1.1
sulpiride	55 ± 5.2	38 ± 6.4	43 ± 13	36 ± 4.68	23 ± 2.99	43 ± 13

[a] Sample: a mixture of seven compounds with a wide range of fractions unbound and diverse structures. A concentration of 5 μM for each compound in all the homogenates was used. Dialysis time 20 h; CV from 10 to 30% in most cases. f_u% refers to the original tissue after conversion using the eq 1. Dilution was prepared by 1:3 brain tissue volume:buffer volume to yield 4-times diluted homogenate and so on.

purpose of this study, we selected a mixture of diverse compounds with a wide range of fraction unbound based on a principal component analysis score. As shown in Table 2, the dilution of tissue homogenate only minimally influenced f_u values. This result is in line with the assumption that drug and tissue binding is governed by hydrophobicity. It was hypothesized that the reversible macromolecular binding of drugs in plasma and tissues is driven by the main binding molecules present in these two matrices.[26] As phospholipid concentration are present in overwhelming excess,[26] drugs may primarily partition into phospholipids, while other macromolecules present in tissue matrices would contribute insignificantly due to much lower concentrations. Our data suggest that a nearly consistent f_u in brain tissue should be expected up to at least 20-fold tissue dilution.

3.3. Effect of Dialysis Time on Fraction Unbound. For practical reasons, we usually dialyze samples overnight (18−20 h) for measurement of f_u for plasma protein binding as well as brain homogenate binding. Other laboratories, however, have used shorter dialysis times. We therefore compared the effect of dialysis time on fraction unbound using mouse brain homogenate. In comparison of f_u data dialyzed at 4.5 and 20 h, it seems that fractions unbound measured at 4.5 h are somewhat higher than those obtained from overnight dialysis for a majority of compounds examined, nevertheless resulting in an overall good correlation (Table 1). Recovery and stability of all compounds were examined without significant differences between 4.5 h and overnight. In general, a short dialysis time of 4 h often attains equilibrium.[24] However, compounds requiring more than 6 h to reach equilibrium have also been demonstrated.[27] Our study based on the set of 25 compounds suggests no significant difference of f_u between 4.5 and 20 h. However, from the viewpoint of the best scientific performance and practice, a longer dialysis time such as 20 h is often conducted in our lab, unless stability data suggest otherwise.

Correlation of Brain f_u between Single Compound Measurement and Pooled Compounds. Table 1 summarizes f_u data measured by sample pooling (all 25 compounds pooled in one sample) and conventional single compound measurement from published data in mouse brain tissue. Figure 2 shows a strong correlation ($R^2 = 0.906$, $n = 25$) of f_u between single compound measurement and measurement of 25 pooled compounds. It should be emphasized that the above correlation is based on data generated from two different laboratories as well as slightly different homogenate dilutions. As indicated in Figure 2, a 2-fold difference in f_u was observed in the worst cases of chloropromazine (with a basic pK_a 9.54) and carisprodol (neutral), though it does not seem that basic compounds tend to bind more to phospolipid than neutral compounds. Such variability should be acceptable for screening purposes. In addition, in order to examine the potential ion suppression effect, a comparison of the total 25 pooled compounds versus selectively pooled compounds with baseline resolutions was made. A tight correlation ($R^2 = 0.9651$, $n = 25$) was obtained between all 25 pooled compounds and selected pooled compounds, indicating that overlapped peaks or incomplete chromatographic resolutions

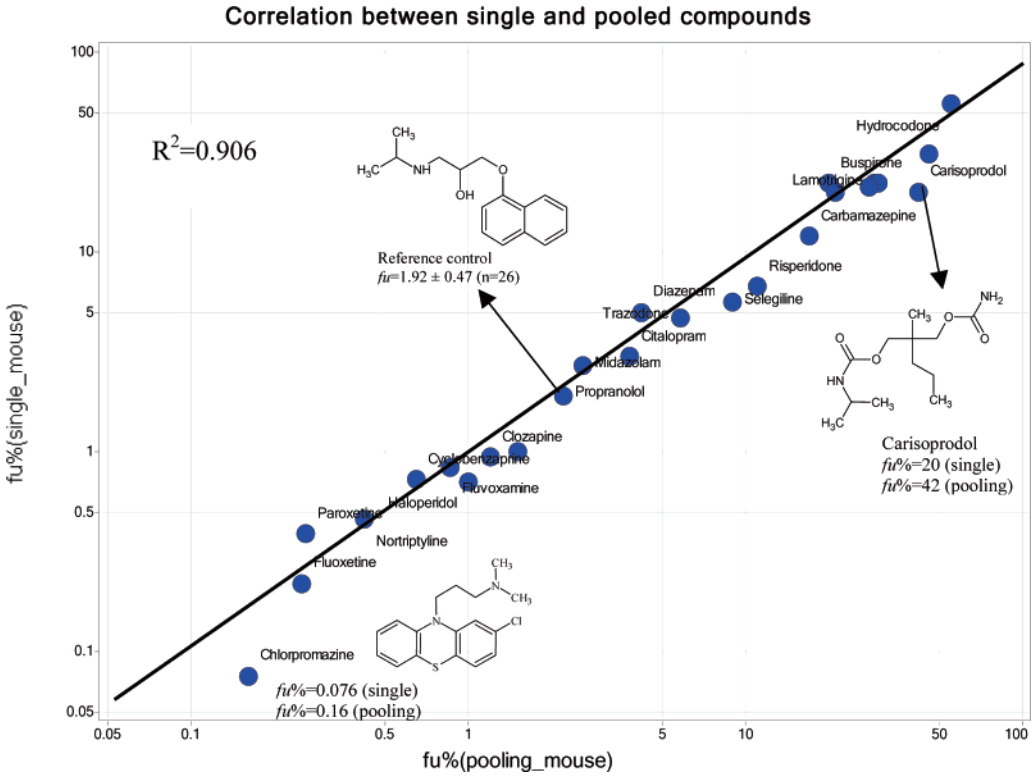

Figure 2. Correlation of f_u between single compound measurement and pooled compounds. f_u(single) data taken from ref 12. f_u(pooling) data measured in this work by pooling 25 compounds in a single sample. The concentration of each compound is 4 μM in the homogenate. Dialysis time was 4.5 h. The f_u(single) datum for propranolol is the mean value ($f_u = 1.92 \pm 0.47$) of all 26 measurements from five different batches of mouse brain tissues (the lowest and highest f_u observed are 1.3% and 2.8%, respectively), which acts as a reference control for the whole assay.

have a negligible effect on f_u. Current results suggest that up to 25 compounds can be pooled and dialyzed and simultaneously measured, affording f_u values very close to those obtained with conventional single compound measurements. In addition, a comparison with fresh and frozen (kept in freezer at −20 °C for more than 4 months) mouse tissue was conducted using the same set of pooled compounds resulting in similar f_u values ($R^2 = 0.9089$, $n = 25$). This result, combined with the data obtained with different batches of tissues, confirms that a robust and reproducible f_u can be obtained by the sample pooling approach as long as tissue homogenate samples are appropriately collected, prepared, and stored. It is worthwhile mentioning that another distinct advantage of the sample pooling approach is that f_u screening data can be ensured, since the compounds of interest are always measured along with the reference compound (in our case propranolol) under the same conditions. As exemplified in Figure 2 for propranolol, a statistical mean value from all 26 measurements ($f_u = 1.92 \pm 0.47$; the lowest f_u and highest f_u are 1.3 and 2.8, respectively) from the five different batches of mouse tissues can be utilized for assay control.

3.5. Comparison of Mouse and Rat Brain Tissue Binding and Estimation of Tissue Binding. As mouse and rat are the most frequently used animals for evaluation of in vivo pharmacological effect, it is interesting to compare whether drugs bind or partition to mouse and rat brain tissues to different degrees. Using the sample pooling approach, the unbound fractions were measured for the same set of compounds in both mouse and rat brain homogenates. As shown in Figure 3, a tight correlation ($R^2 = 0.9887$, $n = 25$) of f_u between rat and mouse brain tissues was observed. This result is well in accordance with the average lipid contents in tissues where the phospholipid content (fractional content of wet tissue weight 0.0532) and neutral lipid (0.031) in mouse brain tissue are equivalent to those in rat brain tissue, i.e., 0.05 and 0.0393,[26] supporting the theoretical nonspecific binding model (eq 4−6). It is worthwhile noting that similar f_u in rat and guinea pig brain tissues has been observed, although only three compounds were shown.[13] This implies that f_u measured in mouse brain tissue can be used for interpretation of pharmacokinetic and pharmacodynamic data in the rat. On the basis of the above observation and a general nonspecific binding mechanism, the fraction unbound in tissue y (f_{u-y}) can thus be estimated by measured f_{u-x} in tissue x by eq 8, which combines the lipid contents in respective tissues.

$$f_{u-y} = \frac{f_{u-x}}{\left(\frac{\text{lipid}_y}{\text{lipid}_x}\right) - \left(\frac{\text{lipid}_y}{\text{lipid}_x} - 1\right) f_{u-x}} \quad (8)$$

In order to confirm that the proposed approach is generic and applicable to various tissues, f_u values in adrenal, brain, lung, and brown fat from rat for two AZ compounds along with reference compound propranolol were investigated, respectively. As shown in Table 3, a decrease in lipophilicity results in increased fractions unbound, which is consistent for all examined tissues. For all three compounds, the same trend in increase of fractions unbound was observed from adrenal gland, brain, lung to brown fat tissues, most likely attributed to the decreased lipid contents present in the respective tissues. As demonstrated in Table 3, a good correlation was obtained between measured f_u in lung tissue and calculated f_u by the proposed eq 8 using measured f_u in rat brain tissue and fractional phospholipid contents in both rat brain and lung tissues, revealing that a nonspecific binding mechanism is driving the partitioning of drug in tissues by predominated hydrophobic interactions between drug and lipids. In other terms, such partitioning in a particular tissue could be estimated by the available lipid content from the tissues. The current approach will have an important

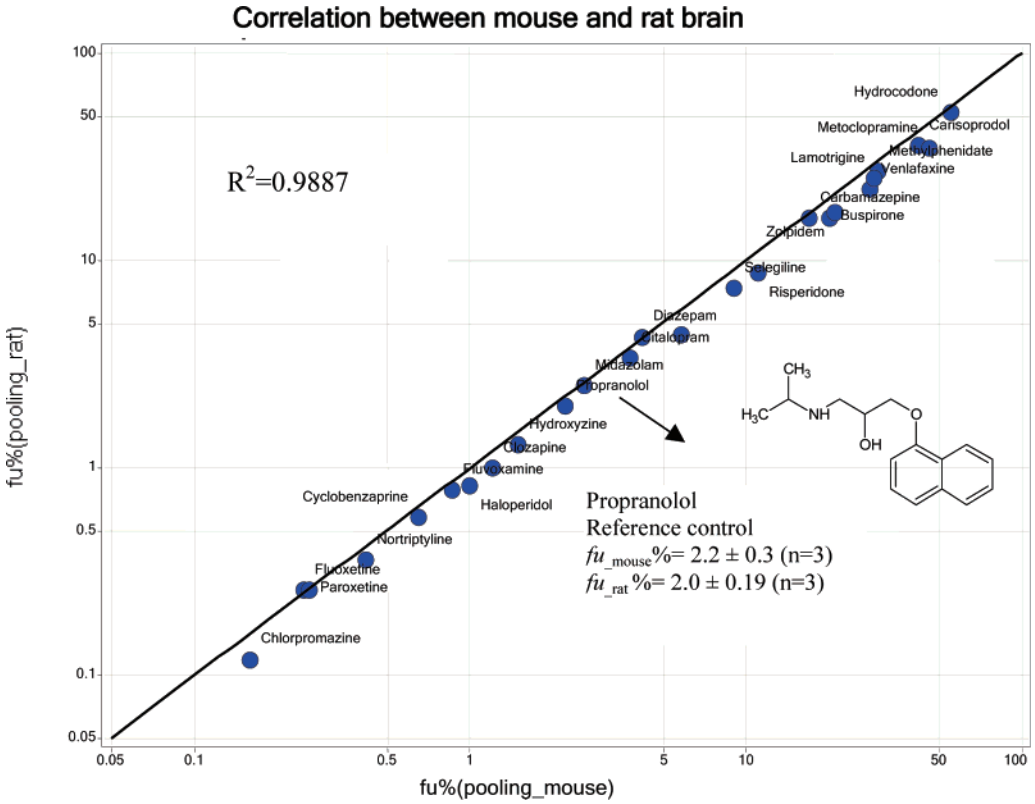

Figure 3. Consistent f_u between rat and mouse brain homogenate. Data obtained from a total of 25 mixed compounds using mouse and rat brain homogenates (1:3 volume tissue:volume buffer). Dialysis time was 4.5 h. The propranolol is the reference control compound in this work. The consistence of f_u brain in both mouse and rat tissues corresponds to the phospholipid contents in the respective tissues.[26]

Table 3. Measured f_u in Various Rat Organs and Calculated f_u in Lung Tissue[a]

	lipophilicity		f_u%(measured)				f_u%(cald):[b]
compound	k' (capacity factor)	ACDlogD7.4	adrenal gland	brain	lung	brown fat	lung
AZ_1	12.4	3.96	0.0051 ± 0.0009	0.024 ± 0.0076	0.11 ± 0.068	0.17 ± 0.072	0.074
AZ_2	11.1	3.88	0.25 ± 0.083	1.0 ± 0.15	2.2 ± 0.44	2.8 ± 0.48	3
propranolol	9.3	1.35	1.0 ± 0.14	2.1 ± 0.60	5.3 ± 0.69	9.7 ± 1.56	6.2
phospholipid content				0.053[c]	0.017[c]		

[a] Rat brain homogenates used were diluted 4 times (1:3 volume tissue:volume buffer) for f_u%(measured) ($n = 2$). Dialysis time was 20 h. Other tissues were also from rat with identical homogenization. [b] Calculation based on the eq 8 using measured rat brain f_u and fractional lipid contents in the brain and lung tissues (only fractional phospholipid content concerned taken into account as an approximation for calculation). [c] Data taken from ref 26.

implication to a better understanding and development of new physiologically based pharmacokinetic models (PBPK) by means of more easily accessible tissue binding data using a simple estimation approach across species. For the PBPK modeling, the tissue−blood partitioning coefficients of the drug in various organs and tissues need to be known.[28] Due to limited availability of $f_{u-tissue}$ data, $f_{u-tissue}$ binding has been assumed either by setting $f_{u-tissue}$ as 1 or taking $f_{u-tissue}/f_{u-plasma}$ ratio as 0.5 in the PBPK prediction models.[26,29] So far, little is known about the factors underlying brain tissue binding, and in vitro and in silico measures are usually necessary due to labor-intensive and low-throughput in vivo techniques.[2] There are few comparisons between homogenate and slice binding in literature, but the significant correlation between slice and homogenate binding has been reported.[30] A recent study on 15 diverse structures has demonstrated a reasonably good correlation between f_u in vitro homogenate or slice and f_u in vivo using microdialysis technique.[31] These results suggest that the in vitro binding data f_u in brain should be relevant and supportive for the in vivo estimation of the binding property of drugs in brain.

3.6. Relationship between Fraction Unbound in Tissues and Molecular Structure. A total of 108 compounds were employed in order to analyze structure−brain f_u relationships and derive statistical models. These include 25 commercial CNS compounds as detailed in Table 1 as well as 83 AZ proprietary compounds, acting at different CNS targets, as shown in Figure 4. The AstraZeneca molecules originated from three different drug discovery projects and represent sets of close analogues from seven diverse chemical series.

Simple one-variable analysis shows that there is a good correlation between unbound brain and plasma fraction values ($r = 0.78$), as outlined in Figure 5. This would suggest that the mechanisms regulating the fraction unbound in brain homogenate for the compounds analyzed here are mainly nonspecific. Our result also supports the most often reported values (the ratio of $f_{u-plasma}/f_{u-tissue} \approx 0.5$,[26]). Additionally, as displayed in Figure 6, a strong inverse relationship ($r = -0.78$) was observed between the unbound brain fraction and lipophilicity, as computed with the Suzuki method.[32] Linear fitting would yield a root-mean-square error (RMSE) in the predictions of 0.6 log units. The plot indicates that increasing hydrophobicity translates in a steady decrease of fraction unbound in the brain tissue. This implies that compounds with ClogP ≤ 3 have an 86% chance to achieve fractions unbound of at least 1%, whereas molecules with ClogP ≥ 4 face an 88.6% risk of having brain f_u smaller than 1%. When only the compounds measured in

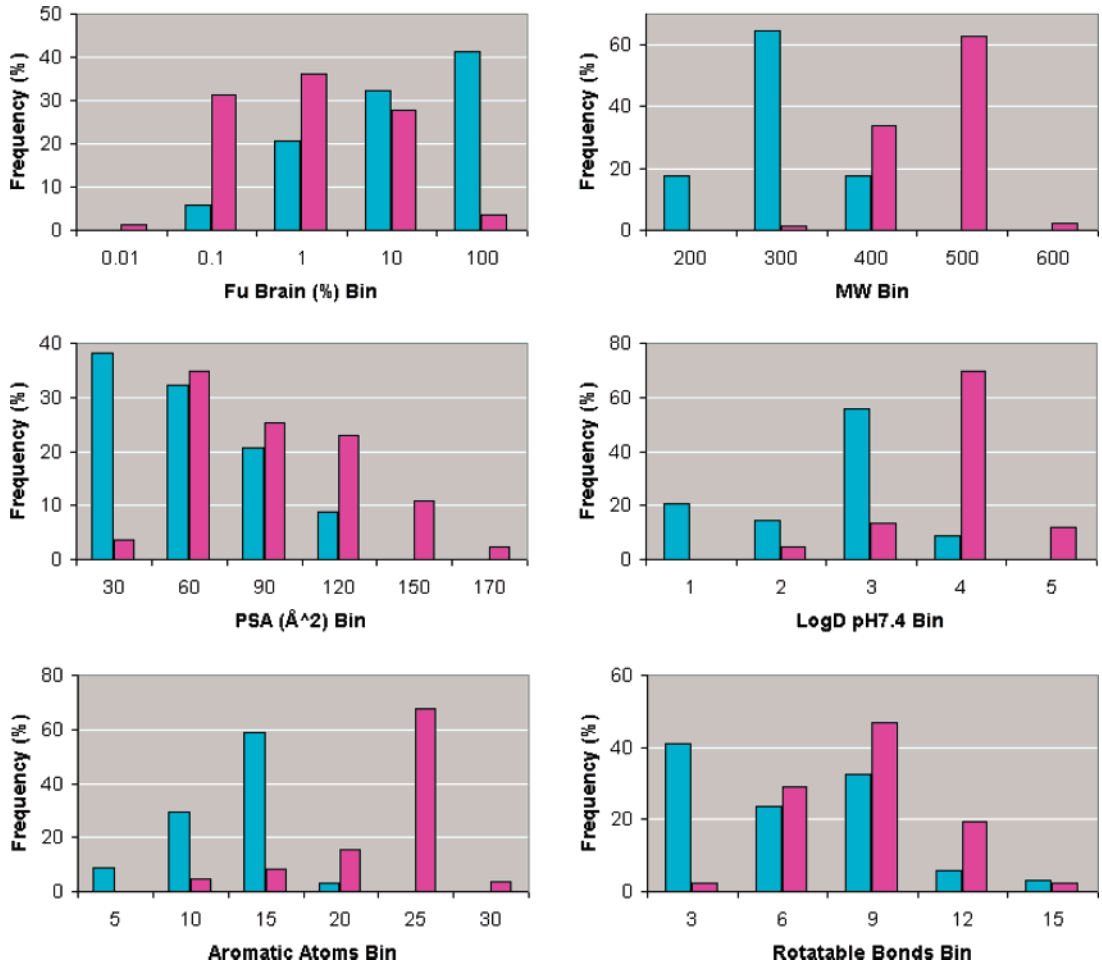

Figure 4. Descriptive statistics for public ($N = 25$, cyan columns) and AZ ($N = 83$, magenta columns) compounds in the present data set. AZ compounds spans seven diverse chemical series from three drug discovery projects.

mouse ($N = 70$) are considered, the trend between brain fraction unbound and ClogP is even more evident ($r = -0.87$, RMSE = 0.54 log units). The mouse data further highlight the physicochemical requirements (ClogP <4) for effective (>1%) fraction unbound.

The observed trends offer robust prediction of f_u in brain tissue. Additionally, they may serve to flag potential problems in lead series in the early phases of drug discovery projects, seeking CNS-active compounds. However, the implicit error in the final predictions would still be on the order of 3−4% brain f_u units. This may clearly pose problems in the late optimization phase, when more precise predictions are needed to guide compound prioritization. We thus investigated whether it was possible to derive more accurate models to predict fraction unbound in brain, using a set of 70 compounds, for which brain f_u was measured in mice. Different statistical methods accounting for both linear and nonlinear effects were evaluated, and the results obtained on the test set observations are reported in Table 4. On the whole, the models had good predictive power, with r^2 values in the 0.74−0.87 range (Table 4). Here, the support vector machine (SVM) model displayed the highest accuracy in the predictions, with a RMSE of 0.36 log unit, as shown in Figure 7. Unsurprisingly, ClogP is the most important parameter in the model, due to its evident relationship with f_u and it seems to be a more relevant descriptor for the models described in this work than measured lipophicity log*D*7.4 obtained from a LC C-18 column. One could anticipate that an alternative lipophilicity measure based on immobilized artificial membrane (phospholipid type) column might improve the correlation with fraction unbound in brain tissue as it consists of phospholipid analogues bonded covalently to silica particles, more resembling the brain tissue matrix. Interestingly, two other structural descriptors seem to play a substantial role in the final predictions. The number of aromatic atoms has a negative influence on f_u, while the solvent accessible polar surface area is positively contributing to f_u. As the solvent accessible polar surface area (SAPSA) was found to be positively correlated to f_u, introduction of polar groups in the molecule is likely to increase its f_u. However, because of their greater accessibility, terminal polar groups would provide a larger contribution to SAPSA than more crowded hydrophilic functions. Interestingly, both the number of aromatic atoms and the solvent-accessible polar area are only weakly correlated ($r < 0.6$) to ClogP and, therefore, they might contribute complementary information to the model.

After the model was derived, eight additional in-house compounds were measured in the f_u assay and they offered an additional prospective test for the SVM model. These molecules included structural neighbors to compounds in the training set ($N = 3$, Tanimoto distance < 0.3) as well as more diverse chemotypes ($N = 5$, Tanimoto distance > 0.3). Gratifyingly, the errors in the predictions (RMSE = 0.37 log units) were still comparable to the ones obtained for the first test set (RMSE = 0.36 log units), suggesting that the SVM model is a robust and accurate estimator of brain f_u. Continual evaluation of the model and incorporation of new measured data will serve to ensure better predictive power and adequate coverage of compound space.[33]

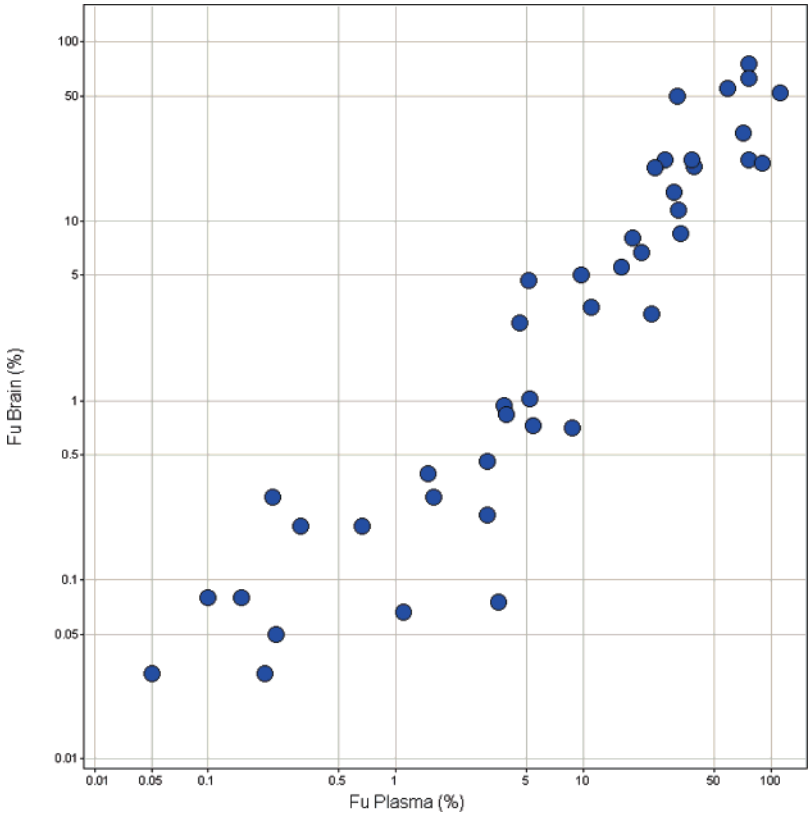

Figure 5. Observed relationship between mouse brain and plasma fractions unbound ($N = 42$, $r = 0.78$).

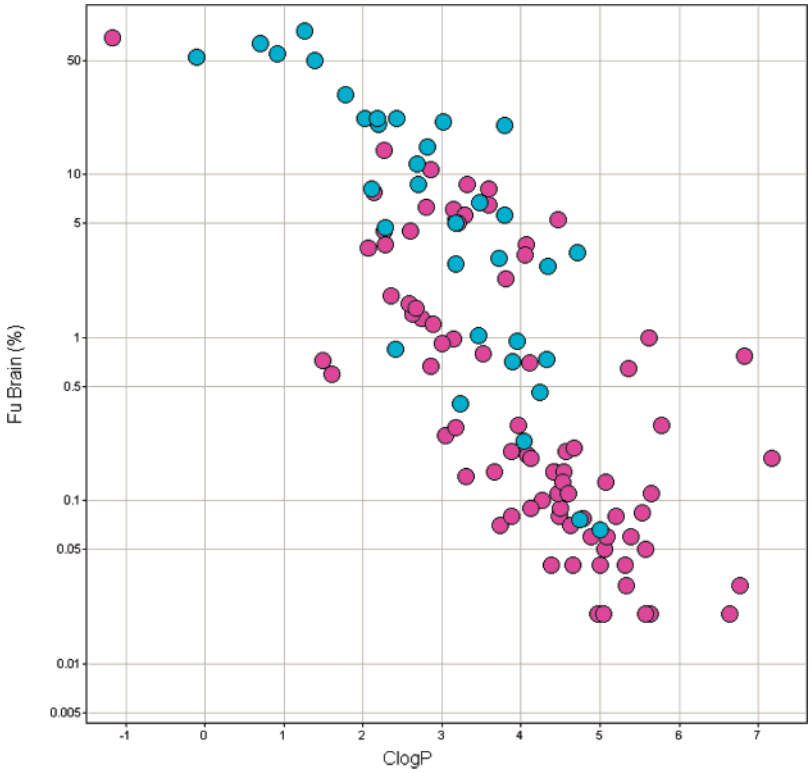

Figure 6. Observed relationship between f_u brain and calculated ClogP[3] [$N = 108$, $r = -0.78$, RMSE = 0.6 log(f_u%)]. Colors as in Figure 4.

4. Conclusions

We have presented a semi-high-throughput method for in vitro screening of drug brain homogenate binding based on a sample-pooling approach using equilibrium dialysis combined with LCMS. This straightforward and robust approach provides a more efficient way to attain unbound brain exposure for the interpretation of in vivo pharmacological effects. In addition to considerably increased throughput, this approach offers other advantages in terms of timesaving and the reduction of cost and tissue volume consumption as well as ensured data quality. We have validated that a set of 25 CNS compounds pooled in one sample led to f_u values in close agreement with conventional

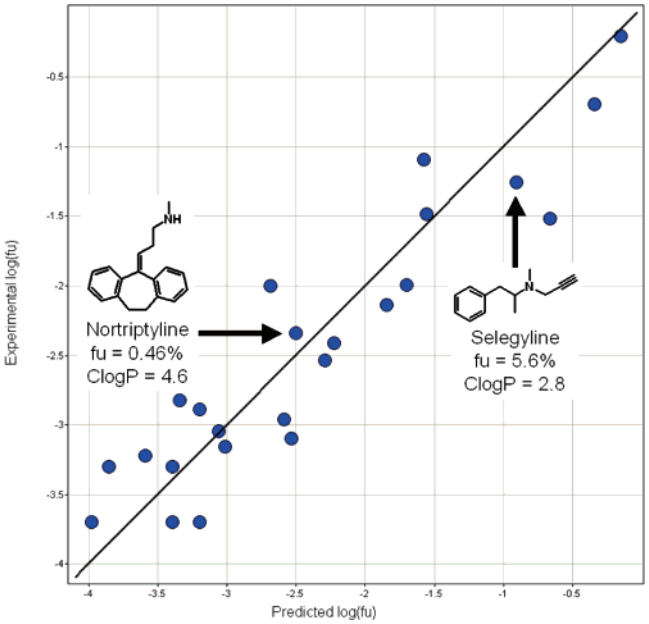

Figure 7. SVM model: experimental vs predicted f_u results for the test set [$N = 24$, $r = -0.871$, RMSE = 0.36 log(f_u%)].

Table 4. Test Set Results for Different QSAR Models Predicting f_u ($N = 24$)

model	method	r^2	RMSE
logP LR	linear regression based on log *P*	0.756	0.54
MLR	multiple linear regression	0.744	0.5
PLS	partial least squares	0.794	0.45
PCR	principal component regression	0.814	0.43
NN	neural network	0.819	0.41
SVM	support vector machine	0.871	0.36

single compound measurements, without apparent ion suppression effect during LCMS bioanalysis. The second important contribution of this work is that the observed consistent f_u in mouse and rat brain tissues suggests no binding or partitioning discrepancy for the two commonly used species in vivo due to the fact that drugs nonspecifically bind mainly to adipose components such as lipids. On the basis of this finding, the extent of drug binding to various tissues can be estimated by the proposed approach utilizing measured f_u from a particular tissue combined with data on the lipid contents, which will provide a simple and fast approach for facilitating PBPK modeling development and validation. Our statistical modeling indicates a strong relationship between lipophilicity and fraction unbound. ClogP can be effectively used as a guideline in the design of compounds with higher f_u. Here, molecules with ClogP > 4 should be treated with caution, as they are very likely to afford f_u less than 1%. On the basis of these findings, a robust QSAR model is also proposed to aid the fine-tuning of f_u. In summary, the proposed new screening method combined with an in silico approach for the rapid assessments of drug tissue binding will benefit CNS target projects.

Acknowledgment. We would like to thank our colleagues Dr. Walter Lindberg, for assistance with lipophilicity measurement and valuable discussions; Anders Holmén, for good comments and providing interesting references; Tord Inghardt, David Morgan, and Lars-Olof Larsson, for their interest and sharing of their valuable experience and knowledge in working with CNS target projects. Lena Svensson and Arja Schedwin are greatly acknowledged for skillful help with brain tissue homogenate preparations. We are also grateful to Markus Fridén and Dr. Ulf Bredberg for valuable comments on the manuscript.

References

(1) Liu, X. R.; Chen, C. P. Strategies to optimize brain penetration in drug discovery. *Curr. Opin. Drug Discovery Dev.* **2005**, *8*, 505−512.
(2) Hitchcock, S. A.; Pennington, L. D. Structure−brain exposure relationships. *J. Med. Chem.* **2006**, *49*, 7559−7583.
(3) Adenot, M.; Lahana, R. Blood-brain barrier permeation models: Discriminating between potential CNS and non-CNS drugs including P-glycoprotein substrates. *J. Chem. Inf. Comput. Sci.* **2004**, *44*, 239−248.
(4) Platts, J. A.; Abraham, M. H.; Zhao, Y. H.; Hersey, A.; Ijaz, L. et al. Correlation and prediction of a large blood-brain distribution data set−An LFER study. *Eur. J. Med. Chem.* **2001**, *36*, 719−730.
(5) Allen, D. D.; Geldenhuys, W. J. Molecular modeling of blood-brain barrier nutrient transporters: In silico basis for evaluation of potential drug delivery to the central nervous system. *Life Sci.* **2006**, *78*, 1029−1033.
(6) Cheng, A.; Diller, D. J.; Dixon, S. L.; Egan, W. J.; Lauri, G. et al. Computation of the physio-chemical properties and data mining of large molecular collections. *J. Comput. Chem.* **2002**, *23*, 172−183.
(7) Ecker, G. F.; Noe, C. R. In silico prediction models for blood-brain barrier permeation. *Curr. Med. Chem.* **2004**, *11*, 1617−1628.
(8) Clark, D. E. Computational prediction of blood-brain barrier permeation. *Annu. Rep. Med. Chem.* **2005**, *40*, 403−415.
(9) Martin, I. Prediction of blood−brain barrier penetration: Are we missing the point? *Drug Discovery Today* **2004**, *9*, 161−162.
(10) Pardridge, W. M. Log(BB), PS products and in silico models of drug brain penetration. *Drug Discovery Today* **2004**, *9*, 392−393.
(11) Doran, A.; Obach, R. S.; Smith, B. J.; Hosea, N. A.; Becker, S. et al. The impact of P-glycoprotein on the disposition of drugs targeted for indications of the central nervous system: Evaluation using the MDR1A/1B knockout mouse model. *Drug Metab. Dispos.* **2005**, *33*, 165−174.
(12) Maurer, T. S.; DeBartolo, D. B.; Tess, D. A.; Scott, D. O. Relationship between exposure and nonspecific binding of thirty-three central nervous system drugs in mice. *Drug Metab. Dispos.* **2005**, *33*, 175−181.
(13) Summerfield, S. G.; Stevens, A. J.; Cutler, L.; Osuna, M. D.; Hammond, B. et al. Improving the in vitro prediction of in vivo central nervous system penetration: Integrating permeability, P-glycoprotein efflux, and free fractions in blood and brain. *J. Pharmacol. Exp. Ther.* **2006**, *316*, 1282−1290.
(14) Kalvass, J. C.; Maurer, T. S.; M., P. G. Use of plasma and brain unbound fractions to assess the extent of brain distribution of 34 drugs: Comparison of unbound concentration ratios to in vivo P-glycoprotein rfflux ratios. *Drug Metab. Dispos.* **2007**, *35*, 660−666.
(15) Lanao, J. M.; Fraile, M. A. Drug tissue distribution: Study methods and therapeutic implications. *Curr. Pharm. Des.* **2005**, *11*, 3829−3845.
(16) Romer, J.; Bickel, M. H. A method to estimate binding constants at variable protein concentrations. *J. Pharm. Pharmacol.* **1979**, *31*, 7−11.
(17) Kalvass, J. C.; Maurer, T. S. Influence of nonspecific brain and plasma binding on CNS exposure: Implications for rational drug discovery. *Biopharm. Drug Dispos.* **2002**, *23*, 327−338.
(18) Wan, H.; Holmen, A. G.; Wang, Y. D.; Lindberg, W.; Englund, M. et al. High-throughput screening of pK, values of pharmaceuticals by pressure-assisted capillary electrophoresis and mass spectrometry. *Rapid Commun. Mass Spectrom.* **2003**, *17*, 2639−2648.
(19) Wan, H.; Thompson, R. A. Capillary electrophoresis technologies for drug screening. *Drug Discovery Today: Technol.* **2005**, *2*, 171−178 (invited review).
(20) Wan, H.; Ulander, J. High-throughput pKa screening and prediction amenable for ADME profiling. *Expert Opin. Drug Metab. Toxicol.* **2006**, *2*, 139−155 (invited review).
(21) http://www.r-project.org, T.R.P.f.S.C.
(22) Pipeline Pilot, v.5; Scitegic, T. C. S., San Diego, CA 92121−4779.
(23) Wan, H.; Rehngren, M. High-throughput screening of protein binding by equilibrium dialysis combined with liquid chromatography and mass spectrometry. *J. Chromatogr.* **2006**, *A 1102*, 125−134.
(24) Lindup, W. E. Plasma protein binding of drugs-some basic and clinical aspects. *Progress in Drug Metabolism*; Taylor & Francis Ltd: Philadelphia, 1987; pp 141−185.
(25) Wan, H.; Bergström, F. High-throughput screening of drug-protein binding in drug discovery. *J. Liq. Chromatogr. Relat. Technol.* **2007**, *30*, 681−700 (invited review).
(26) Poulin, P.; Theil, F. P. A Priori prediction of tissue:plasma partition coefficients of drugs to facilitate the use of physiologically-based pharmacokinetic models in drug discovery. *J. Pharm. Sci.* **2000**, *89*, 16−35.

(27) Banker, M. J.; Clark, T. H.; Williams, J. A. Development and validation of a 96-well equilibrium dialysis apparatus for measuring plasma protein binding. *J. Pharm. Sci.* **2003**, *92*, 967−974.
(28) Bjorkman, S. Prediction of the volume of distribution of a drug: Which tissue−plasma partition coefficients are needed? *J. Pharm. Pharmacol.* **2002**, *54*, 1237−1245.
(29) Poulin, P.; Schoenlein, K.; Theil, F. P. Prediction of adipose tissue: plasma partition coefficients for structurally unrelated drugs. *J. Pharm. Sci.* **2001**, *90*, 436−447.
(30) Liu, X.; Smith, B. J.; Chen, C.; Callegari, E.; Becker, S. L. et al. Use of a physiologically based pharmacokinetic model to study the time to reach brain equilibrium: An experimental analysis of the role of blood−brain barrier permeability, plasma protein binding, and brain tissue binding. *J. Pharmacol. Exp. Ther.* **2005**, *313*, 1254−1262.
(31) Fridén, M.; Gupta, A.; Antonsson, M.; Bredberg, U.; Hammarlund-Udenaes, M. In vitro methods for estimating unbound drug concentrations in the brain interstitial and intracellular fluids. *Drug Metab. Dispos.* 2007 (in press).
(32) Suzuki, T.; Kudo, Y. Automatic log P estimation based on combined additive modeling methods. *J. Comput.-Aided Mol. Des.* **1990**, *4*, 155−198.
(33) Gavaghan, C. L.; Arnby, C. H.; Blomberg, N.; Strandlund, G.; Boyer, S. Development, interpretation and temporal evaluation of a global QSAR of hERG electrophysiology screening data. *J. Comput.-Aided Mol. Des.* **2007**, *21*, 189−206.

JM070375W